Soft Tissue Classification Using Young's Modulus Estimated by the Least Squares Techniques

Pakorn Uttayopas

***Abstract*— In robotic-assisted minimally invasive surgery (RMIS), accurately identifying soft tissues is essential for precision and safety. Traditional geometry-based methods fail due to tissue deformability, while statistical features can be redundant and computationally costly. Mechanical properties like viscoelasticity offer potential but mainly describe resistance to deformation rather than intrinsic characteristics. Young's modulus, on the other hand, provides a well-defined characterization of soft tissue properties, as it considers the relationship between stress and strain, offering a more intrinsic measure of stiffness. Therefore, this study proposes a framework for soft tissue classification using Young's modulus, which quantifies stiffness by relating stress and strain. The estimation was performed using the least squares technique applied to interaction force and position data from haptic exploration. Young's modulus is then used for classification. The method was tested on a robot classifying six phantoms with different mechanical properties, achieving a high classification accuracy of 99.41 ± 0.67% using only a single feature. These results demonstrate that Young's modulus is a promising feature for enhancing accuracy and efficiency in robotic applications in RMIS.**

***Keywords*—** *Robotics; Artificial Intelligence; Man-Machine Interactions*

I. Introduction

In the field of robotic-assisted minimally invasive surgery (RMIS), knowing what an object the robot interacts with is critical to the success of the procedure. For example, during palpation, it is essential to understand the tissue's characteristics and identify the type of tissue the robot is interacting with. This identification could help ensure a safer and more precise procedure that minimizes the risk of tissue damage.

Typically, objects can be identified using geometric features such as shape, size, and contour [1]-[3]. However, they may not be well-suited for identifying soft tissues, as their shape can deform during mechanical interactions. Haptic signals like interaction force and vibration have been successfully used for compliant object classification by extracting statistical features such as mean, minimum, and maximum [4]-[6]. However, this approach depends on specific actions and provide redundant information, potentially affecting classification performance and providing unnecessary high computational cost.

The inherent mechanical properties of objects, which describe their response to a load, provide a specific representation that can be useful for object classification. To classify soft tissue, compliance-related mechanical features like viscoelasticity (stiffness and viscosity) are particularly useful, as they describe how an object deforms under a constant load. These features can be obtained by analyzing the interaction force and object's deformation during an indentation. Such methods empirically estimated stiffness [7], [8], which was successfully used for object classification [5], [9]-[11]. To estimate both stiffness and viscosity, different approaches, such as the least squares method [12]-[14], a Gaussian process [15], and an extended Kalman filters [16], have been used and the estimation results was used for the recognition of various objects in [16], [17].

Young's modulus also describes the intrinsic stiffness of a material. Unlike viscoelasticity, which only measures the material's resistance to deformation, Young's modulus provides a more comprehensive measure by relating stress and strain under an applied load [18], [19]. This may present as another potential feature to improve the recognition and classification of soft tissues, enhancing the accuracy and efficiency of robotic systems in medical applications.

To estimate Young's modulus, the most common approach is to perform a tensile test by measuring the stress and strain of the material to determine the slope [20]. Alternatively, several techniques have been used, such as the Oberst beam technique [21], finite element-based methods [22], [23], and empirical methods [24]. While these estimation methods are effective for industrial applications, they may be too complex for medical applications, where real-time processing and safety are critical.

This prompted us to develop a framework for soft issue classification using Young's modulus as a features. In this framework, the least squares technique, commonly used to estimate parameters in interaction force models like the mass-spring damper, is applied to estimate the Young's modulus of soft tissue. This process uses interaction force and position data obtained from the haptic exploration. Then, we investigate the effectiveness of using only Young's modulus to classify phantoms with various mechanical properties, assuming they represent soft tissues. The results are compared with statistical features and other mechanical features estimated using the least squares method.

Figure 1 illustrates the proposed framework, consisting of two main components: estimation and recognition. A robot

Pakorn Uttayopas is with the Department of Mechanical Engineering, Faculty of Engineering, Thammasat School of Engineering, Thammasat University, Pathum Thani, TH (e-mail: upakorn@engr.tu.ac.th).

interacts with objects to obtain an interaction force data at various locations by indentation. Based on the obtained data, the robot's estimator then calculates the Young's modulus using the least squares method. Following the haptic exploration, the estimated Young's modulus is fed as inputs

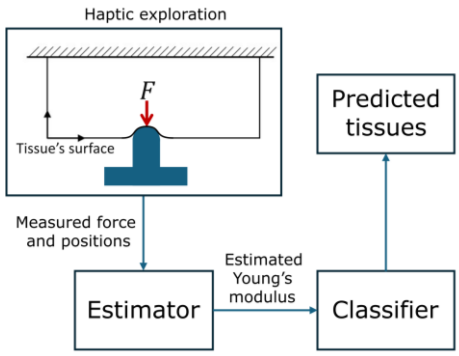

into the object recognition algorithm for classification of soft tissue.

Figure 1. Object recognition process.

II. YOUNG'S MODULUS ESTIMATION

This section describes how the estimation of object's Young's modulus was done. Firstly, an interaction mode is introduced to capture the robot-soft tissue interaction. Using the model, the estimation of the Young's modulus is presented.

A. Interaction model

Let the dynamics of a robot interacting with its environment be described as in [16]:

$$M(q)\ddot{x} + C(q,\dot{q}) + G(q) = u + F + \omega \qquad (1)$$

where x is the end-effector's coordinate and q is the joint angel vector. $M(q)$ and $C(q,\dot{q})$ are inertia and Coriolis matrices while $G(q)$ is the gravitational vector. u is the control input, ω is motor noise. In this work, the contact force is applied by a spherical indentation tip in the normal direction. Thus, the interaction with soft tissue is considered in a single DOF, and can be modeled using Young's (elastic) modulus as in [18]:

$$F = \frac{8E\sqrt{rx}}{3(1+\upsilon)}x + F_0 \qquad (2)$$

where E is Young's modulus, υ is the Poisson's ratio of the phantom, r is the indenter radius, and F_0 the force corresponding to the surface's rest length at x_0 (without interaction).

B. An estimation approach

The E and F_0 in the equation (2) can be estimated using the measured normal force and the end-effector's positions. To simplify the interaction force model, we assumed that υ is constant and known; thus, the equation can be rewritten in the form:

$$F = Ex_{est} + F_0\,, \quad \text{where } x_{est} = \frac{8\sqrt{r}}{3(1+\upsilon)}x^{\frac{3}{2}}. \qquad (3)$$

This means that the nonlinear parameters are transformed into a linear problem. Thus, the least squares method can be used to find the solutions [25]. We denote y as observed valuable which the measured force F, the equation become

$$y = \theta\Phi,\quad \theta = [E\ F_0],\ \Phi = [x_{est}\ 1]^T \qquad (4)$$

where θ is parameters vector to be estimated and Φ is the design matrix containing input values. θ can be estimated using equation (4) as following:

$$\hat{\theta} = (\Phi^T\Phi)^{-1}\Phi^T y \qquad (5)$$

where $\hat{\theta}$ represents the estimated parameters, aiming to minimize the difference from the actual parameter values, θ.

C. Experimental setup

To obtain the interaction force and end-effector position for estimating Young's modulus, the HMan robot [26], a 2-DOF cable-driven planar robot, was used (Figure 2a). A finger with spherical tip radius of $r = 0.01\ m$ was installed on the base of the robot's end-effector, with a six-axis force sensor (SI-25-0.25; ATI Industrial Automation) placed between the tip and the robot's finger base to measure the interaction force in the normal direction (Figure 2b) with a 1 kHz sampling rate.

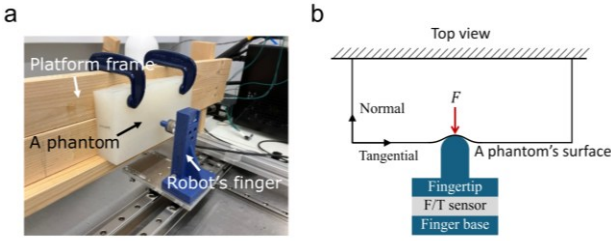

Figure 2. Experimental setup. *(a) Hman robot with a sensorizes finger and a phantom (b) Diagram of robot's finger interating with a phantom.*

The robot performed indentation with six phantoms, each having a relatively flat surface to minimize the shape's influence, as shown in Figure 2a. The phantom were made by a silicone to represent soft tissue (Poisson's ratio $\upsilon = 0.5$) [27]. Table I shows that some phantom share similar viscoelasticity properties creating ambiguous in their classification. The robot's finger pressed against a phantom's surface in the normal direction with desired trajectories $x = 0.01\sin(8\tau) + 0.01\ m,\ \tau \in (0,1]\ s$. The interaction force and end-effector position in the normal direction were collected 25 repetitions of the haptic interaction for each phantom.

TABLE I. MEAN VALUES AND THEIR SD OVER 25 MEASUREMENTS OF VISCOELASTICITY ESTIMATED USING LEAST SQUARES FIT OF A LINEAR SPRING-DAMPER MODEL.

Phantoms	*Stiffness (N/m)*	*Viscosity (Ns/m)*
Hard silicone	722.30 ± 30.65	8.025 ± 0.76
Mediumn hard silicone	505.30 ± 32.38	8.01 ± 0.93
Slightly hard silicone	384.86 ± 36.48	14.36 ± 1.68
Slightly soft silicone	293.46 ± 18.38	9.98 ± 0.58
Medium soft silicone	239.36 ± 20.01	10.22 ± 1.27
Soft silicone	162.36 ± 6.89	11.49 ± 0.45

D. Estimation results

Table II shows the estimated Young's modulus resulting from the equation (5) using the measured interaction force and the end-effector's position. Unsurprisingly, the results show that softer phantoms have lower Young's modulus values, while stiffer phantoms have higher values. Furthermore, the results show distinct differences in Young's modulus values, providing sufficient variability in object classification.

TABLE II. MEAN VALUES AND THEIR SD OVER 25 MEASUREMENTS OF YOUNG'S MODULUS ESTIMATED USING LEAST SQUARES FIT OF THE YOUNG'S MODULUS MODEL.

Phantoms	*Young's modulus (kPa)*
Hard silicone	48.63 ± 0.63
Mediumn hard silicone	35.42 ± 0.85
Slightly hard silicone	20.01 ± 0.62
Slightly soft silicone	15.26 ± 0.32
Medium soft silicone	12.75 ± 0.51
Soft silicone	7.67 ± 0.12

III. PHANTOM CLASSIFICATION

The classification was performed using the experimental data in Section III with Young's modulus used as a feature for phantom classification. To highlight the benefits of this feature, the classification results were compared with those obtained using a different set of features.

A. Alternative feature sets

Traditionally, statistical features were extracted from the raw force and position data as a function of time. These include the mean, maximum value, minimum value, root mean square (RMS), and standard deviation (SD), all calculated over time in the normal direction for both the interaction force and end-effector position, totaling 11 features.

The interaction force in equation (1) can be modeled as a linear mass-spring-damper system to describe phantom behavior during haptic interaction. The stiffness and viscosity parameters can be estimated using the least squares method, based on end-effector's position and velocity, and the interaction force. These estimated parameters are then used as features to represent the phantom's mechanical properties.

Alternatively, the interaction force can be modeled nonlinearly using the Bouc-Wen model [28]. As presented in [29], the least squares method can be used to estimate three parameters that represent internal stiffness and control the hysteresis loop. These parameters, estimated from end-effector's position and velocity and the interaction force, were used as additional features for phantom classification.

In summary, four features sets are formed based on the force and position data as shown in Table III.

TABLE III. FEATURE SETS USED FOR PHANTOM CLASSIFICAITON

Denomination	*Features*
YM: Young's modulus	Estimated Young's modulus
L-MP: Linear mechanical properties	Estimated stiffness and viscosity
NL-MP: Nonlinear mechanical properties	3 estimated nonlinear parameters in the Bouc-Wen model
SF: Statistical features	11 statistical features

B. Classification approach

The Naive Bayes classifier was used to predict the phantom's class based on the training feature set. It calculates the posterior probability of a class, c given the feature set O_n using Bayes' Theorem:

$$P(c|O_n) = \frac{P(O_n|c)P(c)}{P(O_n)} \quad (6)$$

where $P(c|O_n)$ is the likelihood, $P(c)$ is prior beliefs of class c and $P(O_n|c)$ is probability of feature set O_n. The predicted object c^* is the class that maximize the posterior probability:

$$c^* = \arg\max_{c \in C} P(c|O_n). \quad (7)$$

The classification was performed on 50 simulation runs for each features sets, with training and testing feature sets in a 1:1 ratio.

C. Results Analysis

A statistical test was carried out to examine the significance of the improvement achieved by our method compared to other feature sets. The Shapiro-Wilk test verified that the classification results followed a normal distribution across all groups, allowing for the application of a one-way ANOVA. Subsequently, t-tests were conducted for post-hoc analysis.

D. Classification Results

Figure 3 shows that using Young's modulus as a feature resulted in a classification accuracy of 99.41 ± 0.67%. Some confusion occurred between phantom medium soft silicone and slightly soft silicone, accounting for a 0.59% error. However, this error is relatively small compared to the overall results.

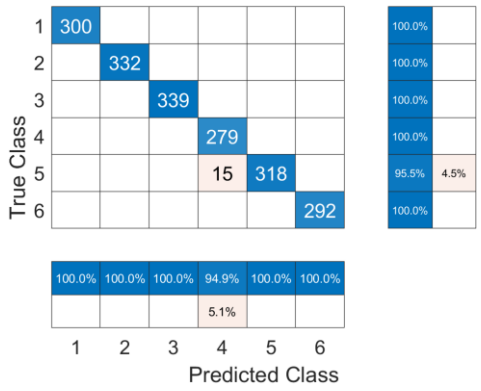

Figure 3. Confusion matrix obtained by using the estimated Young's modulus

E. *Comparison of Classification Results*

Figure 4 shows classification results using YM, L-MP, NL-MP and SF. Using Young's modulus as a feature resulted in a classification accuracy of 99.41 ± 0.67 %. In comparison, linear mechanical properties (stiffness and viscosity) from the mass-spring-damper model achieved 96.56 ± 1.99 %. The Bouc-Wen model's estimated parameters yielded 93.73 ± 2.95 while statistical features provided 95.68 ± 5.56 %. These results indicate that using only Young's modulus as a feature achieved the highest classification accuracy with the lowest variance (lowest SD), showing a significant difference from the other feature sets (t-test with $p > 0.05$).

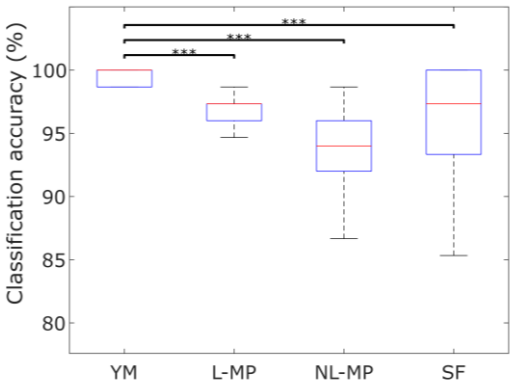

Figure 4. Comparison of classificaiton accuray, *the classification results obtained using different feature sets described in Table III.*

IV. Discussion & Conclusion

This work presents a phantom classification method based on the estimation of the soft tissue Young's modulus. The Young's modulus was estimated using the least squares technique, utilizing the interaction force and indentation position in the normal direction. The estimation was demonstrated using experimental data obtained through indentation, and the results show potential for representing the unique properties of each phantom. These findings could be valuable for phantom classification.

The classification was performed using the obtained experimental data. Using only the estimated Young's modulus as a feature yielded a classification accuracy of 99.41 ± 0.67 %. This result is higher than those obtained using L-MP, NL-MP, and SF, which contain 2, 3, and 11 features, respectively. These findings suggest that Young's modulus is highly informative for distinguishing the different mechanical properties of the phantom, even with only a single feature. Thus, the proposed approach offers lower computational costs during classification.

Young's modulus provided lower variance in classification results than L-MP, NL-MP, and SF, indicating it is more robust than the other features. This may be because L-MP and NL-MP require both position and velocity, increasing input complexity and potential noise, while Young's modulus only requires position. Additionally, the linearization method in NL-MP can lead to inconsistent results and poor parameter estimation. SF depends on specific actions and can be redundant, leading to greater variance in classification results.

Although the obtained results are promising, some limitations should be acknowledged. As a proof of concept, the interaction model used in this work is relatively simple and only considers the normal direction. More sophisticated models, including both tangential and shear directions, should be further explored to provide more comprehensive information about the phantom. Furthermore, the proposed approach was primarily tested using flat-surface phantoms to minimize the influence of shape on the results. For more complex and irregular surfaces phantoms resembling biological tissues, the proposed approach should be extended by integrating a contour-following algorithm into the controller.

In summary, Young's modulus effectively represents a phantom's properties and can be used to classify phantoms with different mechanical properties. This is critical in haptic interactions during robot- systems, where maneuvers need to be carefully planned based on the interacting objects. For example, a stiffness map generated from object properties can help identify tumours and guide surgical procedure with greater precision, minimizing tissue damage and unnecessary exploration. Lastly, to increase versatility, online estimation should be further investigated with an expanded dataset in future work.

References

[1] P. K. Allen and K. S. Roberts, "Haptic object recognition using a multi-fingered dextrous hand," in IEEE Int. Conf. Robot. Autom., 1989, pp. 342–347.

[2] U. Martinez-Hernandez, T. J. Dodd, and T. J. Prescott, "Feeling the shape: Active exploration behaviors for object recognition with a robotic hand," IEEE Trans. Syst. Man Cybern. Syst, vol. 48, no. 12, pp. 2339–2348, 2018.

[3] H.M.A. van der Werff and F.D. van der Meer, "Shape-based classification of spectrally identical objects", ISPRS Journal of Photogrammetry and Remote Sensing, Vol. 63, no. 2, pp.251-258 2008.

[4] S. Chitta, J. Sturm, M. Piccoli, and W. Burgard, "Tactile sensing for mobile manipulation," IEEE Transactions on Robotics, vol. 27, no. 3, pp. 558–568, 2011.

[5] J. Hoelscher, J. Peters, and T. Hermans, "Evaluation of tactile feature extraction for interactive object recognition," in IEEE-RAS International Conference on Humanoid Robots, 2015, pp. 310–317.

[6] M. Kaboli, K. Yao, D. Feng, and G. Cheng, “Tactile-based active object discrimination and target object search in an unknown workspace,” Autonomous Robots, vol. 43, no. 1, 123–152, 2019.

[7] Z. Su, J. Fishel, T. Yamamoto, and G. Loeb, “Use of tactile feedback to control exploratory movements to characterize object compliance,” Frontiers in Neurorobotics, vol. 6, p. 7, 2012.

[8] M. Bednarek, P. Kicki, J. Bednarek, and K. Walas, “Gaining a sense of touch object stiffness estimation using a soft gripper and neural networks,” Electronics, vol. 10, no. 1, 2021.

[9] D. Xu, G. E. Loeb, and J. A. Fishel, “Tactile identification of objects using Bayesian exploration,” in IEEE Int. Conf. Robot. Autom., 2013, pp. 3056–3061.

[10] A. J. Spiers, M. V. Liarokapis, B. Calli, and A. M. Dollar, “Single-grasp object classification and feature extraction with simple robot hands and tactile sensors,” IEEE Transactions on Haptics, vol. 9, no. 2, pp. 207–220, 2016.

[11] S. Chitta, J. Sturm, M. Piccoli, and W. Burgard, “Tactile sensing for mobile manipulation,” IEEE Transactions on Robotics, vol. 27, no. 3, pp. 558–568, 2011.

[12] L. Love and W. Book, “Environment estimation for enhanced impedance control,” in IEEE Int. Conf. Robot. Autom., vol. 2, 1995, 1854–1859.

[13] R. Rossi, L. Fossali, A. Novazzi, L. Bascetta, and P. Rocco, “Implicit force control for an industrial robot based on stiffness estimation and compensation during motion,” IEEE Int. Conf. Robot. Autom., pp. 1138–1145, 2016.

[14] A. Ren, C. Qi, F. Gao, X. Zhao, and Q. Sun, “Contact stiffness identification with delay and structural compensation for hardware-in-the-loop contact simulator,” Journal of Intelligent and Robotic Systems, vol. 86, pp. 1–9, 2017.

[15] P. Chalasani, L. Wang, R. Yasin, N. Simaan, and R. H. Taylor, “Preliminary evaluation of an online estimation method for organ geometry and tissue stiffness,” IEEE Robotics and Automation Letters, vol. 3, no. 3, pp. 1816–1823, 2018.

[16] P. Uttayopas, X. Cheng, J. Eden, and E. Burdet, “Object recognition using mechanical impact, viscoelasticity, and surface friction during interaction,” IEEE Transactions on Haptics, vol. 16, no. 2, pp. 251–260, 2023.

[17] K. Yane and T. Nozaki, “Recognition of environmental impedance configuration by neural network using time-series contact state response,” in IEEE International Conference on Advanced Motion Control, 2022, pp. 426–431.

[18] E. H. Lee and J. R. M. Radok, “The contact problem for viscoelastic bodies,” Journal of Applied Mechanics, vol. 27, no. 3, pp. 438–444, Sep. 1960.

[19] C. T. McKee, J. A. Last, P. Russell, and C. J. Murphy, “Indentation versus tensile measurements of young’s modulus for soft biological tissues,” Tissue Engineering Part B: Reviews, vol. 17, no. 3, pp. 155–164, 2011.

[20] F. P. Beer, E. R. Johnston, J. T. Dewolf, and D. F. Mazurek, “Mechanics of Materials”, 6th ed., McGraw-Hill Companies, New York, 2012.

[21] Y. Liao and V. Wells, “Estimation of complex young’s modulus of non-stiff materials using a modified Oberst beam technique,” Journal of Sound and Vibration, vol. 316, no. 1, pp. 87–100, 2008.

[22] S. M. Haddad, S. S. Dhaliwal, B. W. Rotenberg, A. Samani, and H. M. Ladak, “Estimation of the young’s moduli of fresh human oropharyngeal soft tissues using indentation testing,” Journal of the Mechanical Behavior of Biomedical Materials, vol. 86, pp. 352–358, 2018.

[23] A. P. C. Choi and Y. P. Zheng, "Estimation of Young's modulus and Poisson's ratio of soft tissue from indentation using two different-sized indentors: Finite element analysis of the finite deformation effect," Medical & Biological Engineering & Computing, vol. 43, pp. 258–264, 2005.

[24] X. Peng, J. Huang, L. Qin, *et al.*, “A method to determine Young’s modulus of soft gels for cell adhesion,” Acta Mechanica Sinica., vol. 25, pp. 565–570, 2009.

[25] Michael L. Johnson, Lindsay M. Faunt, “Parameter estimation by least-squares methods,” Methods in Enzymology, Academic Press, vol. 210, pp. 1-37, 1992

[26] D. Campolo, P. Tommasino, K. Gamage, J. Klein, C. M. Hughes, and L. Masia, “H-man: A planar, h-shape cabled differential robotic manipulandum for experiments on human motor control,” Journal of Neuroscience Methods, vol. 235, pp. 285–297, 2014.

[27] J. Guo, B. Xiao, and H. Ren, "Compensating uncertainties in force sensing for robotic-assisted palpation," Appl. Sci., vol. 9, no. 12, p. 2573, 2019.

[28] R. Bouc, "Forced vibration of mechanical systems with hysteresis," in Proc. 4th Conf. Nonlinear Oscillations, Prague, Czechoslovakia, 1967, pp. 315–315.

[29] X. Zhu and X. Lu, “Parametric identification of bouc-wen model and its application in mild steel damper modeling,” Procedia Engineering, vol. 14, pp. 318–324, 2011.